

## GRID EROSION MODELING OF THE NEXT ION THRUSTER OPTICS

Jerold W. Emhoff\*  
Iain D. Boyd†

Department of Aerospace Engineering  
University of Michigan, Ann Arbor, MI 48109

### ABSTRACT

Results from several different computational studies of the NEXT ion thruster optics are presented. A study of the effect of beam voltage on accelerator grid aperture wall erosion shows a non-monotonic, complex behavior. Comparison to experimental performance data indicates improvements in simulation of the accelerator grid current, as well as very good agreement with other quantities. Also examined is the effect of ion optics choice on the thruster life, showing that TAG optics provide better margin against electron backstreaming than NSTAR optics. The model is used to predict the change in performance with increasing accelerator grid voltage, showing that although the current collected on the accel grid downstream face increases, the erosion rate decreases. A study is presented for varying doubly-ionized xenon current fraction. The results show that computed performance data is not very sensitive to the current fraction.

### INTRODUCTION

The success of the NSTAR ion thruster in the Deep Space One mission<sup>1</sup> has led NASA to develop a new thruster based on NSTAR technology. The aim is to design a thruster able to process more power and provide a higher total impulse than the NSTAR thruster, enabling even longer and more ambitious missions than Deep Space One. NASA's Evolutionary Xenon Thruster<sup>2</sup>, or NEXT, is a 40 cm thruster, giving approximately twice as much beam extraction area as NSTAR's 30 cm beam diameter. Also, as shown in Soulas et al<sup>3</sup>, a redesigned discharge chamber gives a much flatter beam current density profile. The larger beam diameter and flatter beam profile combine to provide more thrust, while reducing the amount of ion optics erosion. Higher beam voltages are also used in the NEXT thruster, giving greater efficiencies than those seen in the NSTAR thruster. The ion optics geometry is largely the same as in the NSTAR thruster, although two optics sets with different accelerator grid thicknesses are under consideration. The first optics set, referred to as the NSTAR optics, has the same accelerator grid thickness as in the NSTAR thruster. The second optics set has an accelerator grid with 50% greater thickness than NSTAR, called the Thick-Accelerator-Grid (TAG) optics<sup>4</sup>.

---

\*AIAA Student Member, Graduate Student Research Assistant

† AIAA Associate Fellow, Professor

Ion optics modeling is being conducted to aid in the design process of the NEXT thruster. Determining the life of an ion thruster experimentally is a difficult, costly, and lengthy process. Modeling can give order of magnitude or better life estimates in a relatively short time, and at a low cost. This has special relevance in the case of NEXT, as the consideration of two accelerator grid geometries makes experimental testing even more complex and expensive.

The focus of this paper is on modeling of the NEXT thruster ion optics, considering both NSTAR and TAG accelerator grids. Simulation data from various thruster operating points and with varying simulation parameters are analyzed at NEXT operating conditions. Life estimates and performance results are presented for the maximum operating condition of the NEXT thruster, considering differences between the use of progressive erosion rates and initial erosion rates. Performance changes with varying beam voltage are analyzed and compared to experimental data. The effects on the simulated results of varying accelerator grid voltage as well as varying the doubly-charged ion fraction are also presented.

### MODEL OPERATION

The computational code provides a 2-D axisymmetric simulation of a single aperture in an ion thruster. The grid used is composed of evenly spaced rectangular cells. The optics of the thruster are simulated using boundary cells in the domain. These cells may be arranged in an irregular way, allowing the simulation of cusps on the barrels of the grids. A typical computational domain is shown in Figure 1.

The code uses the Particle-In-Cell<sup>5</sup> (PIC) method to simulate xenon ions, xenon neutrals, and doubly-charged xenon ions. Each computational particle has a numerical weight which indicates the actual number of atoms represented by the particle. Flow field quantities for each cell are obtained by averaging the properties of all the particles in the cell, taking into account the weight of each particle. The potential field accelerates ions self-consistently. Electrons are modeled as a fluid, and the Poisson equation is solved using the Alternating-Direction Implicit (ADI) method. Electron densities are retrieved from the potential using the Boltzmann relation. The direct simulation Monte Carlo (DSMC) method<sup>6</sup> is used for processing particle collisions. Both charge exchange (CEX) and momentum exchange collision types are simulated.

To run a simulation, the beamlet current and mass flow rate must first be determined. This is performed by running short simulations with approximately 3 mm computational domain length downstream of the optics, and no included back pressure. This allows relatively quick determination of the necessary input ion and neutral densities. Once the correct densities are determined, the downstream domain length is increased to approximately 2 cm, and back pressure effects are included. The effect of tank or back pressure is modeled by injection of neutral xenon at the downstream boundary. No ions are injected at the downstream boundary.

The simulation begins by operating at a large time-step with only neutral particles in the domain. This allows the slow moving neutrals to rapidly reach a steady state flow. Once a steady-state is reached, ions are injected at the upstream boundary with the Bohm velocity and the input density corresponding to the desired beamlet current. At this point, the time-step is decreased so that the ions are not able to cross more than one cell boundary in a single iteration, maintaining stability.

A typical simulation has approximately 500,000 particles. About 180,000 of these are singly charged ions and 300,000 are neutrals. There are also on the order of ten thousand doubly charged ions. For a typical domain size, about 18,000 iterations are needed to initialize the neutral particle flow, followed by approximately 60,000 iterations to initialize the mixed ion-neutral flow before sampling begins. Once a steady flow has been reached, data is sampled from the simulation over a large number of time-steps, typically on the order of 100,000. On a 1.5 GHz Pentium IV PC, a typical simulation has a running time of approximately two days.

### **SIMULATION RESULTS**

Four sets of simulation data are presented here. First, aperture wall erosion is examined for both NSTAR and TAG optics, considering the effect of progressively enlarging the aperture diameter. Next, results are presented for varying beam voltages at the beam current of 3.1 A and compared to experimental results. Results for varying accelerator grid voltage are then given, followed by simulation data for varying doubly-charged ion current fraction.

#### **Accelerator Grid Wall Erosion Study**

Two of the primary failure modes of an ion thruster are electron backstreaming due to enlargement of the accelerator grid aperture and structural failure of the optics due to erosion on the downstream surface of the accelerator grid. A 2-D simulation cannot capture the

nuances of the structural failure mode however, so the aperture wall erosion is the main focus here. The operating point used is at a total beam current of 3.52 A and a beam voltage of 1800 V. This is the operating point used for wear testing of the NEXT thruster. In all simulations, the beamlet at the radial center of the optics is modeled, giving a beamlet current of 0.186 mA. Also, both NSTAR and TAG optics are simulated for each operating point. The accelerator grid aperture diameter is varied over several runs for both sets of optics, starting with the initial cusped geometry, and ending with a diameter close to the electron backstreaming limit.

To determine the electron backstreaming behavior of the optics, several shortened simulations are performed. In these simulations, no neutrals are included and the domain length downstream of the accelerator grid is maintained at 3 mm. The accelerator grid aperture diameter is varied in each simulation, giving a minimum centerline potential for each configuration. The ion densities injected at the upstream boundary are not changed, so there is some variation in beamlet current. The minimum centerline potential determines whether or not electron backstreaming occurs. If this potential is nearly the same as the downstream plasma potential, electrons can then easily flow into the discharge chamber. This destroys the performance of the thruster. The downstream plasma potential is measured experimentally. Using the erosion rates obtained from the full simulations, the accelerator grid aperture radius can be determined as a function of time. This is then combined with the data for centerline potential and the mass flow rate at the operating point to determine what mass of xenon gas the thruster can process before electron backstreaming occurs.

Figure 2 shows the erosion rate on the barrel and downstream face of the accelerator grid as a function of aperture diameter, for both NSTAR and TAG optics. For both geometries, the erosion rate on the barrel decreases slightly at the beginning of life, followed by a significant increase as the aperture enlarges further. The erosion rate on the downstream face increases near beginning of life, then drops as the aperture diameter increases. The end effect is that the total erosion rate rises slightly for the NSTAR geometry, and remains approximately constant for TAG geometry. As Figure 3 shows, the total current on the grids rises monotonically in both cases, indicating that more CEX ions are being created.

This change in impact location and increase in current can be explained by examining the beamlet focusing as the accelerator grid aperture diameter changes. As the diameter increases, the beamlet becomes less focused,

resulting in a wider region with a high CEX collision rate downstream of the optics. This will create more CEX ions in the downstream region, increasing the number of ions impacting on the downstream face of the accelerator grid, and hence increasing both the current and erosion rate on the downstream surface. The enlargement of the aperture also initially allows more high energy CEX ions created upstream of the accelerator grid to pass through the grid without impacting, leading to a decrease in the erosion rate on the grid barrel. However, as the aperture diameter increases further, the actual area available for impact by ions on the downstream face will decrease, so that more ions created in the downstream region will impact on the barrel, resulting in an increased erosion rate and current.

Figure 4 shows the prediction for thruster life based on the erosion rate data. Electron backstreaming occurs at the 22 V line, and the desired propellant mass throughput before end of life is 400 kg. Two predictions are made—one uses only the initial erosion rate to predict the end of life, while the other prediction uses the erosion rates evaluated as the aperture enlarges. This approach is taken to estimate the accuracy of using only the initial erosion rate, as well as to determine whether it would over or under-predict the mass throughput. It is apparent that use of only the initial erosion rate will result in a lower life estimate, although the difference in estimates is much higher for the TAG optics. We can also see that the TAG optics perform much better than the NSTAR optics, providing over 300 kg more mass throughput, and easily reaching the desired 400 kg throughput level. All sets of results predict that the mass throughput target will be reached, however.

#### Beam Voltage Study

For much of the NEXT erosion study, it is assumed that the worst case operating point is at the highest beam voltage and the highest beam current. However, it has been postulated by Brophy et al<sup>7</sup> that it may in fact be the case that the perveance fraction is the true determining factor for maximum erosion rate. The perveance fraction is defined as

$$f_p = \frac{j_b l_e^2}{V_T^{3/2} P_{\max}}$$

$$l_e = \sqrt{(l_g + t_s)^2 + \frac{1}{4} d_s^2}$$

$$P_{\max} = \frac{4\epsilon_0}{9} \left( \frac{2e}{m_i} \right)^{1/2}$$

where  $V_T$  is the beam voltage minus the accelerator grid voltage,  $j_b$  is the current density upstream of the optics,  $l_g$  is the distance between the grids,  $t_s$  is the thickness of the screen grid,  $d_s$  is the diameter of the screen grid aperture,  $e$  is the electric charge,  $m_i$  is the ion mass, and  $\epsilon_0$  is the permittivity of free space. For xenon,  $P_{\max}=4.77 \times 10^{-9} \text{ A/V}^{3/2}$ . Results given by Brophy, et al indicate that there is a minimum point for the ion energy impacting on the accelerator grid barrel, and thus a minimum for the erosion rate, at a perveance fraction of about 0.2. Directly above or below this point, the erosion rate rises sharply; in the higher perveance region, a slight drop is seen in the erosion rate. If this is correct, then the most critical operating point would be at the beam voltage and beam current just above the perveance fraction of 0.2. To test this theory, results from five cases modeled for the NEXT thruster are presented. The 3.1 A beam current operating point at beam voltages of 2100 V, 1800 V, 1567 V, 1396 V, and 1179 V are all simulated using both NSTAR and TAG optics. Also, the 2.7 A beam current, 1021 V beam voltage operating point is modeled. At each operating point, the peak beamlet current is simulated. This is 0.168 mA for the 3.1 A cases, and 0.149 mA for the 2.70 A case.

In Figure 5, the erosion rate on the accelerator grid aperture wall as a function of perveance fraction is shown. There is indeed a peak in the erosion rate as the perveance increases beyond 0.2, however, there is a sharper drop following the increase, so that the 2.70 A case at 1021 V still has a lower erosion rate than the 3.1 A, 1800 V case. The erosion rates for TAG optics are less sensitive to the perveance for low values, but then drop more sharply as the perveance increases than the NSTAR optics. Although the peak erosion rate is just above a perveance fraction of 0.2 as Brophy predicts, the rise from 0.2 is much less dramatic, and the drop in erosion rate as the perveance continues to increase is much more severe than predicted by Brophy. This may be a result of the different models used, or because of differences in the operating conditions simulated. In either case, it seems that determining which operating conditions give the worst case erosion rate is non-trivial. Upon closer examination of the determining factors, this makes sense. The accelerator grid barrel erosion rate is caused by both the energy and the rate of impacting CEX ions. The energy is directly related to the beam voltage, so decreasing the voltage decreases the energy of the CEX ions. However, decreasing the voltage also increases the perveance, so that CEX ions are more likely to be focused onto the aperture wall. This indicates that the worst case erosion will occur at some middle point, where the energy and number of CEX ions combine to give the maximum erosion rate.

Both the simulations performed here, and the results given by Brophy confirm this.

#### Comparison to Experimental Results

Experimental data collected by Soulas et al<sup>8</sup> give the performance of the NEXT thruster at various operating points. Table 1 shows the operating points for the experimental data, taken using the NSTAR optics, as well as the data of interest. The simulated data is evaluated at the peak beamlet for a given operating point, while the experimental data represents the entire thruster. To offset this difference, all simulated results are multiplied by the number of apertures in the thruster, and by the ratio of the peak beamlet current to the average beamlet current. The one exception to this process is the specific impulse, which is not altered. All of the simulated data correspond to the points in the beam voltage study, except for one additional point at a beam current of 3.52 A, with 1800 V beam voltage.

Figure 6 shows the accelerator grid current as a function of beam voltage. The computational results are somewhat lower than the experimental results, although the fact that they are on the same order of magnitude is an improvement over previous results<sup>9</sup>. The model does predict the change in accelerator current with changing beam current fairly well. The jump from the 2.70 A first point on the plot to the 3.1 A second point is approximately the same for both experimental and simulation results. Also, the model predicts the jump in accelerator current seen at the last point, for the 3.52 A, 1800 V beam voltage operating condition. However, the experimental results show a steady increase in accelerator grid current as the beam voltage increases, and this is not seen in the simulation data. This may be because the cusped geometry is not modeled here, or it may possibly be an effect of differences between the modeled operating point and the experimental operating point, such as varying double ion content.

The specific impulse for both experiment and model are shown in Figure 7 as a function of beam voltage. Both sets of data increase linearly with beam voltage. The model results have a slightly different slope however. This may be an effect of using the peak beamlet, or possibly other factors such as double ion fraction. Even so, the comparison to experimental data is very good.

The thrust as a function of beam voltage is shown in Figure 8. Here, the model follows the exact same trend as the experimental data—a linear increase in thrust as the beam voltage increases, as well as increasing thrust with beam current. The underprediction of the thrust is almost certainly due to the usage of only the peak beamlet. Also shown in Figure 8 is a plot of the model

results increased by 15%. These results are almost exactly the same as the experimental results at every point. It follows that the simulated mass flow rate must also require an increase to match the experimental value, because the Isp values already compare well to the experiment. The mass flow rate requires slightly less of an increase, however, because the modeled specific impulse is lower. Examination of the simulation results reveals that an 8% increase is sufficient to match the experimental mass flow rate data.

#### Accelerator Grid Voltage Study

The primary purpose of this study is to determine if any adverse effects occur when the magnitude of the accelerator grid voltage is lowered in the NEXT thruster. A lower voltage will lead to lower impact energies for CEX ions, as well as lower power usage, but other effects may occur which are unexpected.

The voltage applied to the accelerator grid is varied over a series of simulations, with all other quantities held constant. A beamlet current of 0.186 mA, a beam voltage of 1800 V, and cusped geometry is simulated in all cases, with a 8  $\mu$ Torr background pressure and 2 cm downstream domain length. The thrust and specific impulse are not affected by the changing voltage, and the beamlet current drops very slightly as the voltage is increased. Figure 9 shows that the current collected on the downstream face of the accelerator grid increases with increasing voltage. Figure 10 indicates that the erosion rate on the downstream face decreases with increasing accelerator voltage. In both cases, the current and erosion rate on the grid barrel do not change. The fact that the current increases while the erosion rate decreases is somewhat puzzling, but this can be explained by the fact that the ion beamlet is less focused at higher voltages. This gives higher CEX production rates in the downstream region as the voltage increases, resulting in more ion impacts on the grid. However, the accelerating voltage on the CEX ions is decreasing at the same time, so the total energy of the ions impacting on the grid decreases. The total effect is positive, as the grid lifetime is increased with an increased accelerator grid voltage. The only pitfall is that increasing the voltage too much will result in electron backstreaming, and backstreaming will occur earlier as the aperture enlarges. In order to avoid decreasing the thruster life, it is necessary to be able to decrease the voltage again if needed to prevent electron backstreaming.

#### Effect of Doubly-Charged Xenon Current Fraction

The current fraction of doubly-charged xenon ions ( $Xe^{++}$ ) in the ion thruster plume can be very difficult to determine experimentally. It is a critical factor for use

in modeling, however, as the current fraction is usually an input value for a simulation. Simulating a Xe<sup>++</sup> current fraction that is slightly incorrect may possibly give performance results very different from experimental data.

To test this possibility, simulations are performed with varying Xe<sup>++</sup> current fraction, while all other quantities are held constant. A beamlet current of 0.186 mA, a beam voltage of 1800 V, and cusped geometry is used in each simulation. Figure 11 presents the results of these simulations. The thrust and erosion rate both drop linearly as the current fraction is increased, with an approximately 10% drop in thrust from current fractions of zero to 0.45, and a 30% drop in erosion rate over the same range. The specific impulse increases linearly however, rising nearly 10%. The drop in erosion rate is due to lower ion density, as well as lower CEX cross-sections for Xe<sup>++</sup>. The thrust decreases because Xe<sup>++</sup> provides twice as much current as a singly-charged ion, while only increasing the thrust by the square-root of 2. So when the current is held constant, the thrust decreases. The specific impulse increases because the average exit velocity increases, due to the higher velocity Xe<sup>++</sup>.

The rate of change of these quantities is not extremely large, however. Increasing the fraction from 0.1 to 0.15, a 50% increase, changes the erosion rate by less than 5%, and the thrust and Isp only change by less than 2%. This indicates that, while it is important to have fairly accurate experimental data for the Xe<sup>++</sup> current fraction, small errors will produce negligible change in modeled results.

### CONCLUSION

Results from several computational studies were presented in this paper. A study of the erosion of the accelerator grid aperture wall showed that the TAG optics allowed more propellant mass throughput before electron backstreaming occurred than the NSTAR optics. Also, use of the initial erosion rate to determine the life of the thruster gave a lower life prediction than when the erosion rate was evaluated as the aperture diameter increased.

No clear relation was apparent between the erosion and either beam voltage or perveance fraction. While it was seen that the highest beam voltage may not give the highest erosion rate, the lowest beam voltage at a given beam current does not necessarily do so either. Comparison to experimental data was good: the simulation of accelerator grid current has improved, and comparisons to thrust and specific impulse were excellent.

Analysis of performance with varying accelerator grid voltage showed that while the current collected on the grid increased with increasing voltage, the erosion rate decreased, as a result of the beamlet defocusing and lower ion energies. Other performance parameters remained approximately constant.

Reasonable error in the experimentally measured current fraction of doubly-charged ions should have a small effect on modeled results. Performance data changed linearly with the current fraction, but with a low rate of change.

### ACKNOWLEDGEMENT

This work was funded by the NASA Glenn Research Center under grant NAG3-2497 with George Soulas as the technical monitor.

### REFERENCES

- <sup>1</sup> Polk, J. E., Brinza, D., Kakuda, R. Y., Brophy, J. R., Katz, I., Anderson, J. R., Rawlin, V. K., Patterson, M. J., Sovey, J., Hamley, J., "Demonstration of the NSTAR Ion Propulsion System on the Deep Space One Mission," IEPC-01-075, October 2001.
- <sup>2</sup> Patterson, M. J., Foster, J. E., Haag, T. W., Rawlin, V. K., Soulas, G. C., Roman, R. F., "NEXT: NASA's Evolutionary Xenon Thruster," AIAA 2002-3832, July 2002.
- <sup>3</sup> Soulas, G. C., Haag, T. W., Patterson, M. J., "Performance Evaluation of 40 cm Ion Optics for the NEXT Ion Engine," AIAA Paper 2002-3834, July 2002.
- <sup>4</sup> Soulas, G. C., "Improving the Total Impulse Capability of the NSTAR Ion Thruster with Thick-Accelerator-Grid Ion Optics," IEPC-01-081, October 2001.
- <sup>5</sup> Birdsall, C. K. and Langdon, A. B., *Plasma Physics Via Computer Simulation*, Adam Hilger Press, 1991.
- <sup>6</sup> Bird, G. A., *Molecular Gas Dynamics and the Direct Simulation of Gas Flows*, Oxford University Press, 1994.
- <sup>7</sup> Brophy, J. R., Katz, I., Polk, J. E., Anderson, J. R., "Numerical Simulations of Ion Thruster Accelerator Grid Erosion," AIAA Paper 2002-4261, July 2002.
- <sup>8</sup> Personal communication, George Soulas, December 2002.

Table 1. Operating points and data for comparing the model results to experiment. Computational results shown here are multiplied by the number of apertures and the peak-to-average current ratio.

Beam Current (A)		2.7	3.1	3.1	3.1	3.1	3.52
Beam Voltage (V)		1021	1179	1396	1567	1800	1800
Peak-to-Average Current Ratio		0.61	0.62	0.62	0.62	0.62	0.64
Experimental Results	Accel Current (mA)	9.483	11.54	11.68	11.86	12.22	13.50
	Thrust (mN)	137.5	169.4	184.6	195.3	209.6	237.8
	Specific Impulse (s)	3064	3318	3616	3826	4105	4134
Computational Results	Accel Current (mA)	7.248	9.110	8.867	7.920	7.167	9.621
	Thrust (mN)	122.0	149.1	162.7	171.1	181.9	207.5
	Specific Impulse (s)	3092	3297	3566	3776	4006	4021

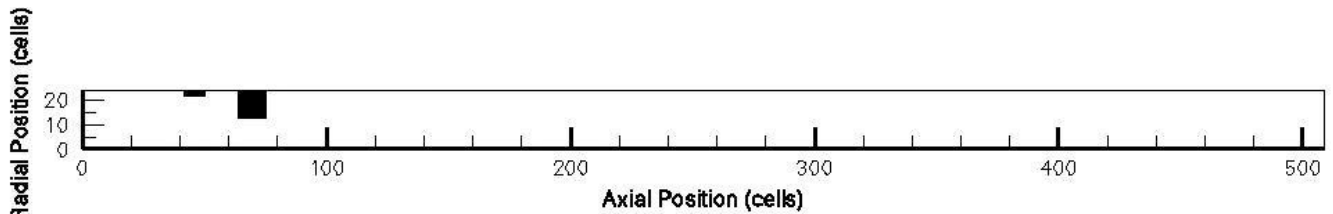


Figure 1. A typical computational domain. The axis numbers represent the number of cells in each direction, and the black areas represent the ion optics.

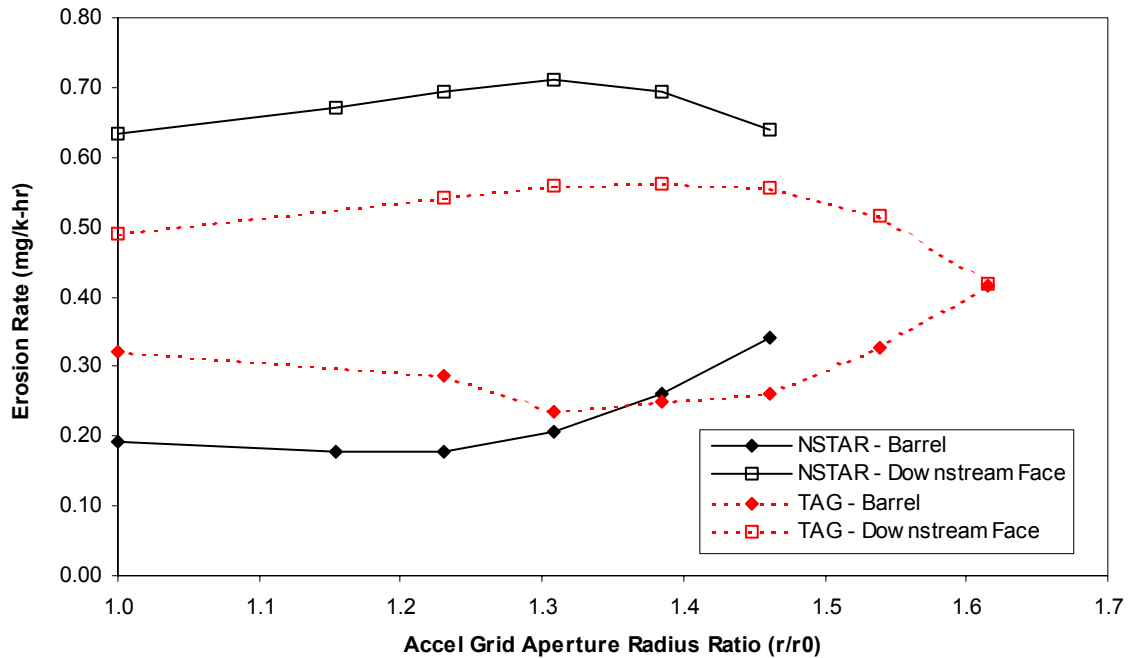


Figure 2. Accelerator grid erosion rate as a function of aperture radius. The erosion rate on the barrel decreases slightly at beginning of life before increasing significantly as the aperture enlarges further.

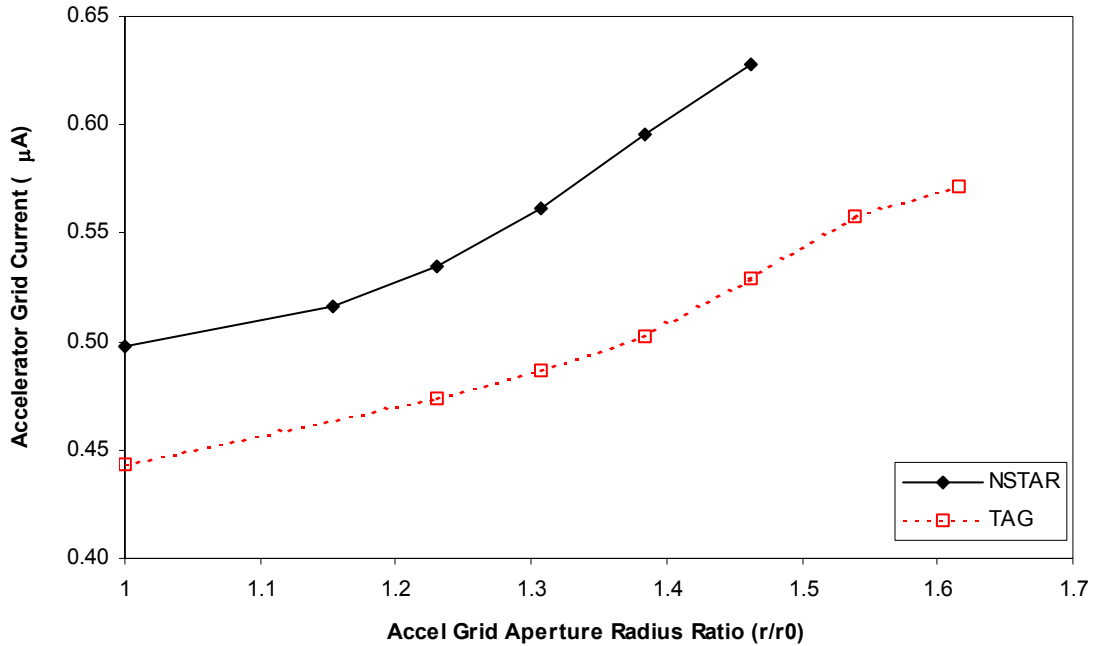


Figure 3. Accelerator grid current as a function of aperture radius. The current increases monotonically with the aperture diameter for both geometries.

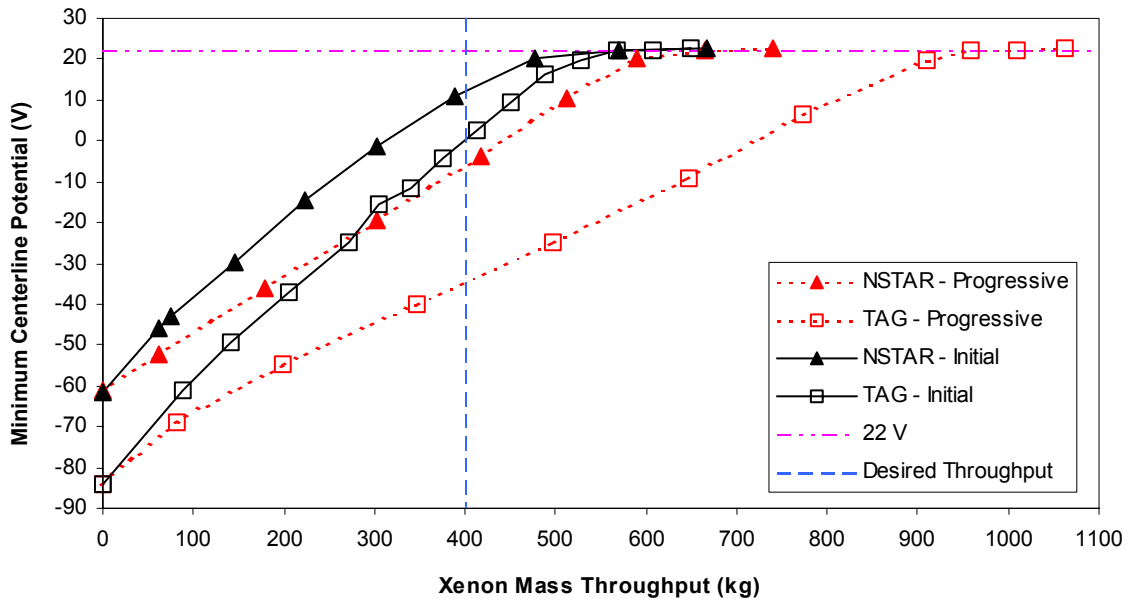


Figure 4. Electron backstreaming prediction for both TAG and NSTAR optics, considering the use of only the initial erosion rate, and the use of progressively determined erosion rates. The TAG optics perform much better than the NSTAR optics, although all cases easily reach the target mass throughput.

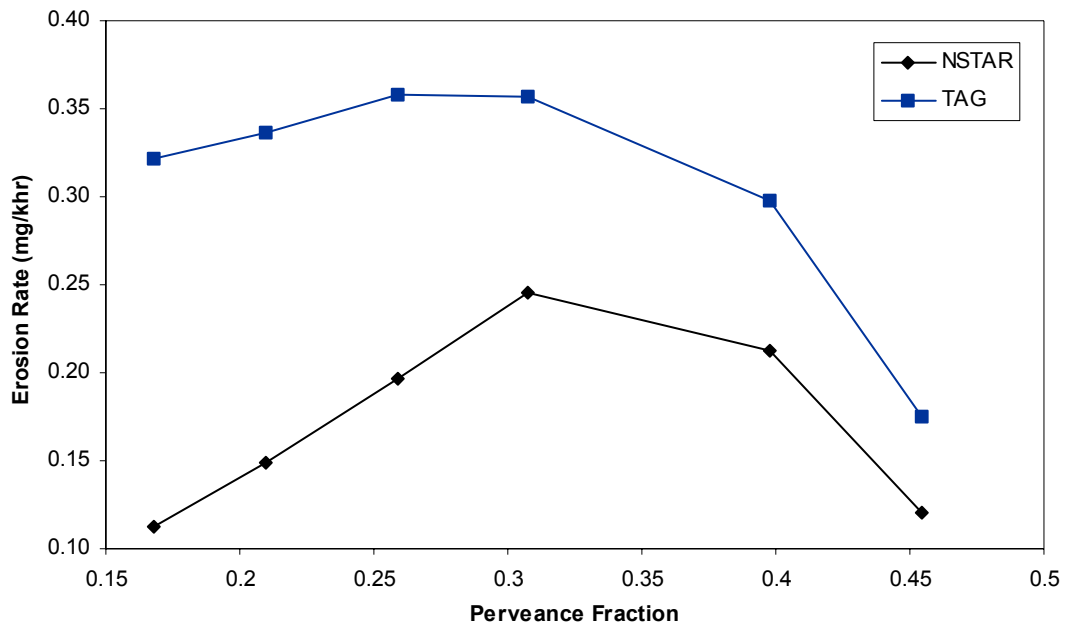


Figure 5. Erosion rate in mg/k-hr as a function of perveance fraction.

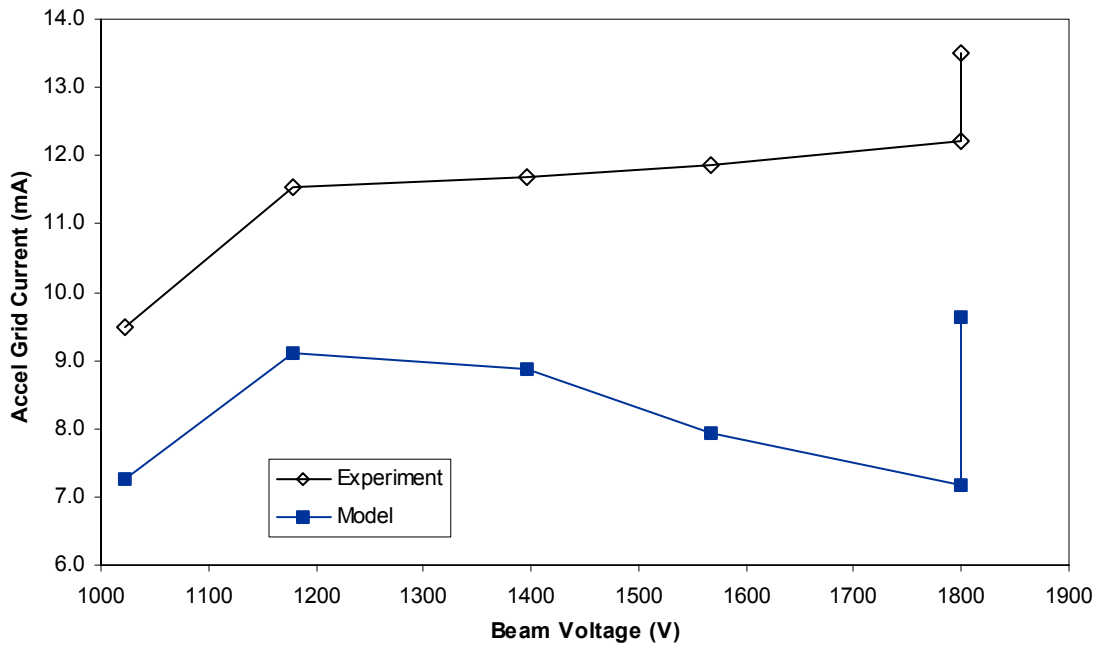


Figure 6. Comparison of experimental data for total accelerator grid current to simulation results, as a function of beam voltage.



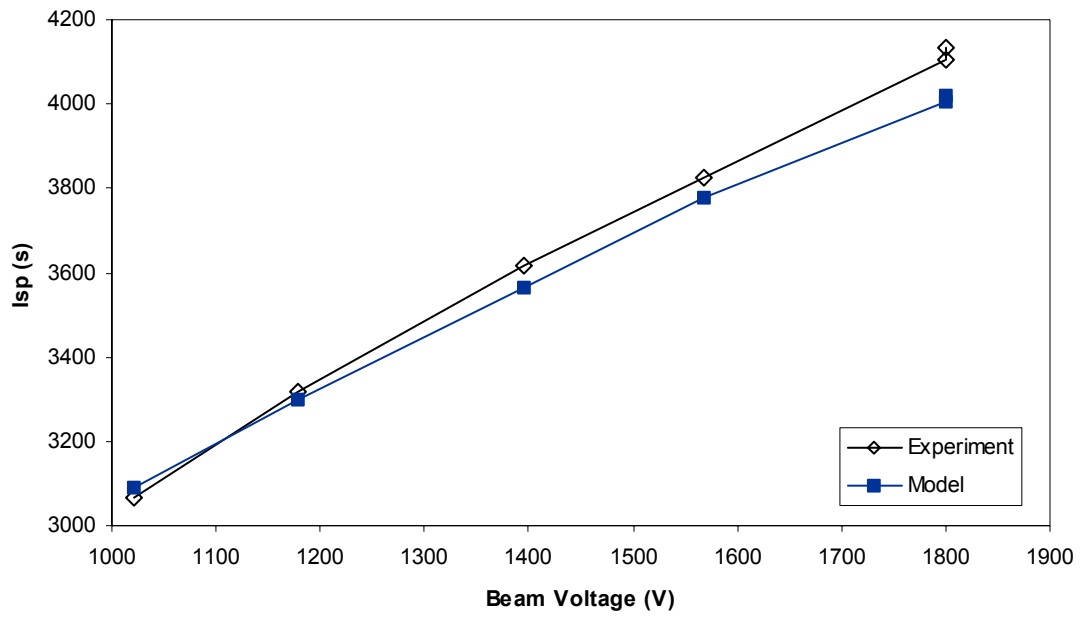


Figure 7. Comparison of experimentally measured specific impulse to simulation results, as a function of beam voltage.

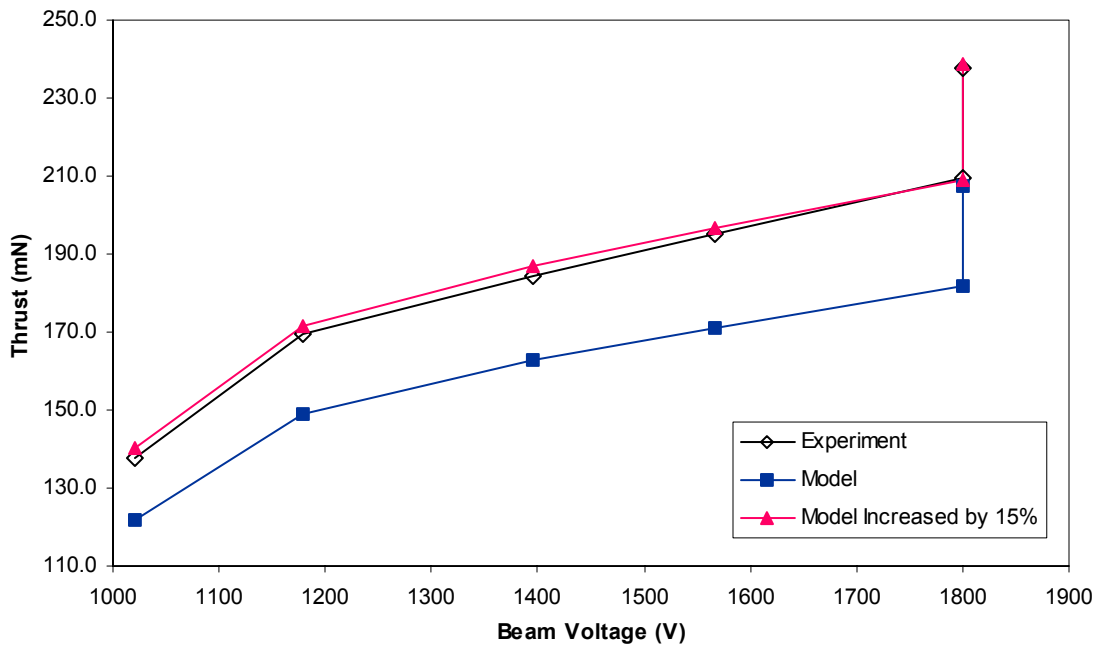


Figure 8. Comparison of experimentally measured thrust to simulation results, as a function of beam voltage. When the model results are increased by 15%, the comparison is almost exact.

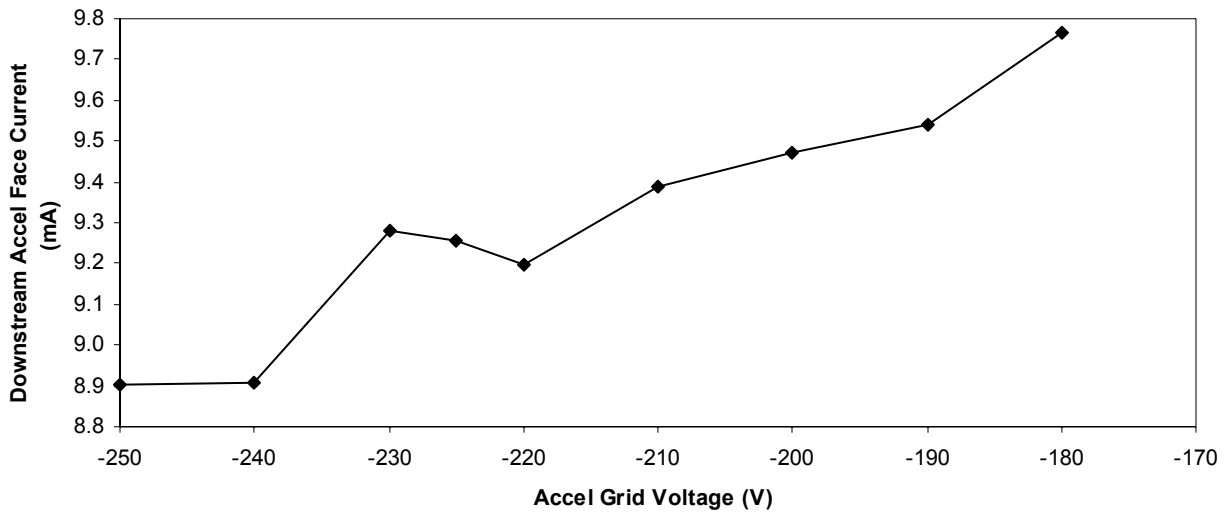


Figure 9. Current collected on the downstream accelerator grid face with varying accelerator grid voltage.

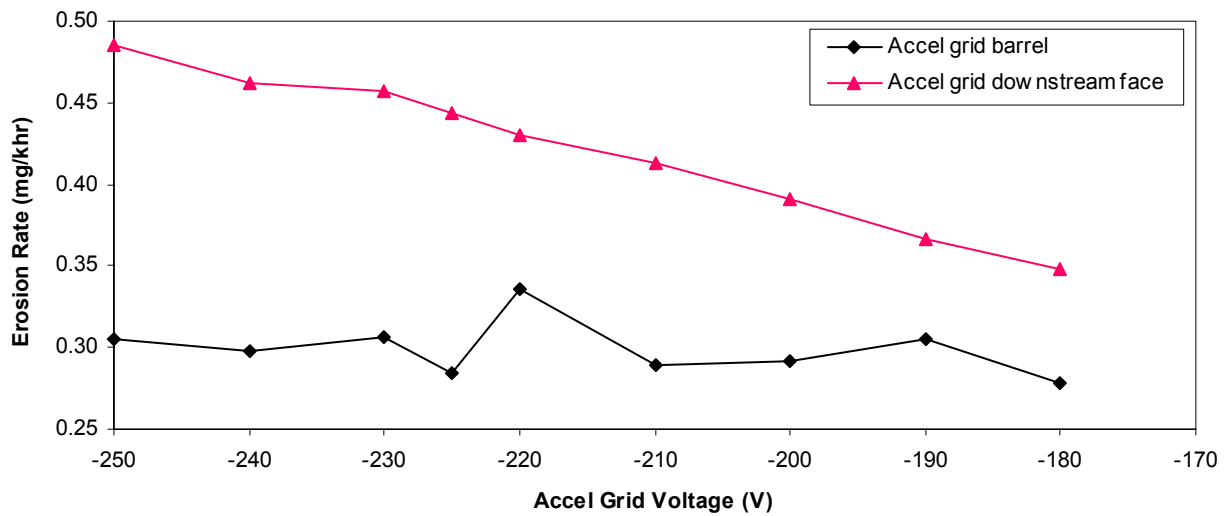


Figure 10. Erosion rate on the downstream accelerator grid face as the accelerator grid voltage is varied.

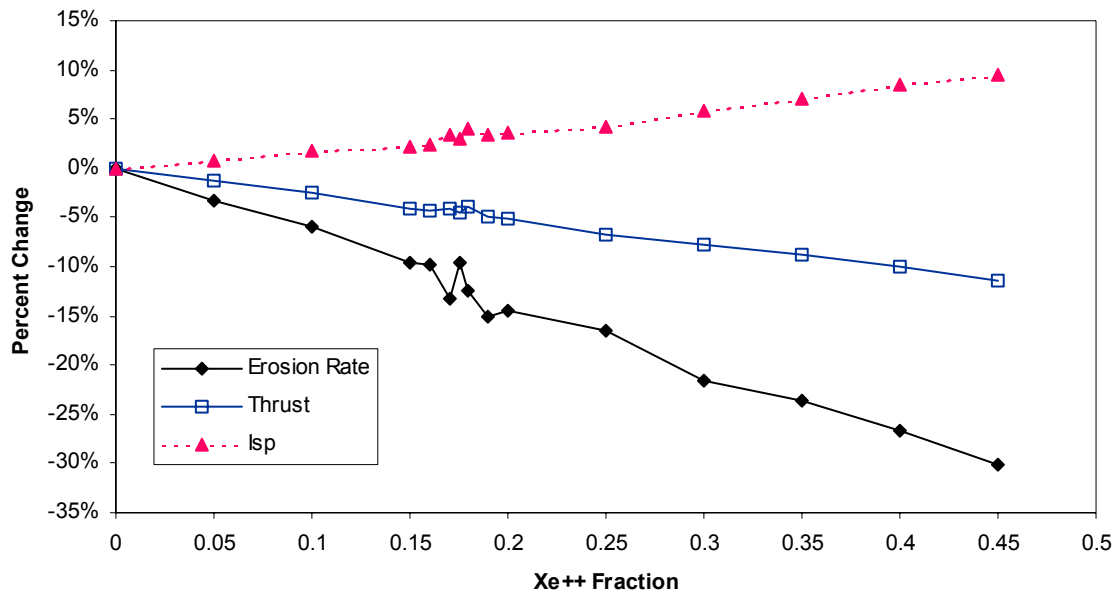


Figure 11. Percent change in performance quantities as a function of doubly-charged ion current fraction.